Met. Mater. Int., Vol. 20, No. 2 (2014), pp. 329~335
doi: 10.1007/s12540-014-1019-8

Study for Corrosion Characteristics of Ferritic Stainless Steel Weld Metal with Respect to Added Contents of Ti and Nb

JongMin Kim and HaeWoo Lee*

Dong-A University, Department of Materials Science and Engineering, 840 Hadan-dong, Saha-gu, Busan 604-714, Republic of Korea

(received date: 30 May 2013 / accepted date: 31 July 2013)

This paper identified the effects of Ti and Nb on pitting and intergranular corrosion resistance in a ferritic stainless steel weld metal of the automobile exhaust system. We fabricated 4 flux cored wires designed with 0-0.2 wt% Ti and 0-1.0 wt% Nb and performed Flux Cored Arc Welding. Through the potentiodynamic polarization test in 0.5M NaCl, we evaluated pitting resistance. And in order to evaluate the intergranular corrosion resistance, we observed microstructure after we performed DL-EPR test in 0.5M H_2SO_4+0.01M KSCN. As a result of the test, the specimen added with 0.2%Ti+1.0%Nb showed the highest pitting resistance. From observing the degree of sensitization and microstructure, the intergranular corrosion resistance was higher as the contents of Ti and Nb increased. And through EBSD we observed Cr carbide which affects the corrosion resistance.

Key words: alloys, welding, corrosion, electron backscattering diffraction (EBSD), scanning electron miscropy (SEM)

1. INTRODUCTION

As there has been a great concern about global warming, people are working on the development of material for the automobile exhaust system and the research for light weight vehicles in order to reduce the air pollution and the automobile exhaust gas. Until now, for materials of the automobile exhaust system, cast iron and etc. have been used widely, but these materials are weak in internal and external corrosion when they are used in severe environments such as in muffler condensate, snow removal calcium chloride, and acid rain etc. Thus, in order to extend the life time of automobile exhaust system parts and raise high performance and environment-friendliness, the use of ferritic stainless steel which has an excellent corrosion resistance has been increased [1-5]. Compared with austenitic stainless steel, ferritic stainless steel used for automobile exhaust system parts is economical because it does not contain expensive nickel. Also, people are developing 400-stainless steel for the high temperature use to which stabilizing elements Ti and Nb are added [6-9]. In general, if stabilizing elements of stainless steel such as Ti or Nb are added to ferritic stainless steel, Ti and Nb are extracted as carbide at high temperature. This can stop the creation of Cr carbide which is formed along with the grain boundary and reduce the sensitization and thus prevent the intergranular corrosion which causes problem in the corrosion resistance [10-15].

Among parts of the automobile exhaust system, a main muffler used at the cold end is the part where the exhaust gas from the engine, and its surface temperature is changed from the room temperature to 400 °C. The uniform internal/external corrosion and the local corrosion accompanied by this heat cycle shall affect the whole parts, and especially the weld metal in which the shape and microstructure is weak and many non-metallic inclusions exist can be damaged severely. For this reason, the corrosion resistance in high temperature is demanded for the weld metal of ferritic stainless steel used for automobile exhaust system parts [5-6].

Therefore, in this study, we evaluated the effect of Ti and Nb upon the corrosion resistance of the weld metal of ferritic stainless steel for the automobile exhaust system used at cold end We prepared 4 specimens of the weld metal by adjusting the contents of Ti and Nb in a flux cored wire and evaluated the effect of the added elements upon the corrosion characteristics of the weld metal by examining pitting corrosion of the weld metal, intergranular corrosion resistance, and microstructure.

2. EXPERIMENTAL PROCEDURES

2.1. Materials and chemical components

For test materials, we prepared 4 specimens by adjusting the amount of Ti and Nb added to the stainless steel flux

*Corresponding author: hwlee@dau.ac.kr

Table 1. Chemical composition of weldmetals

Specimens (wt%)	C	Si	Mn	P	S	Cr	Ti	Nb	Mo	O2	N2
No.1	0.03	0.41	0.48	0.009	0.008	15.8	free	Free	0.61	0.101	0.136
No.2	0.03	0.45	0.52	0.009	0.009	14.9	0.23	Free	0.60	0.104	0.129
No.3	0.03	0.45	0.49	0.010	0.009	14.9	0.21	0.44	0.59	0.109	0.133
No.4	0.03	0.47	0.50	0.011	0.009	15.2	0.24	0.94	0.63	0.101	0.130

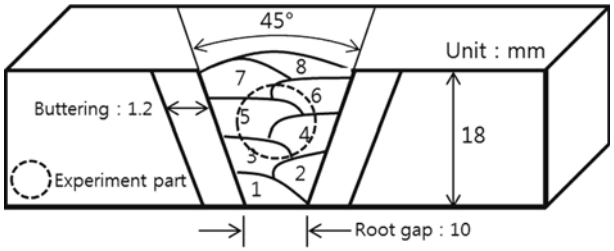

Fig. 1. Schematic diagrams of the weldment.

cored wire components of the existing AISI 436 automobile muffler. The specimens were named as No.1, No.2, No.3, and No.4. To observe the corrosion characteristics with respect to the contents of Ti and Nb, the components of C, Si, Mn, Cr, Mo were fixed, and the content of Ti was adjusted to be 0.2% and Nb to be 0.5% and 1.0%. To measure the chemical components, the optical emission spectrometer (Metal-LAB75/80J, GNR srl, Italy) was used, and the results are shown in Table 1.

2.2. Welding

For welding, as shown in Fig. 1, the buttering with thickness of 1.2 mm was performed in SM490 steel to minimize the effect of the base metal upon the deposited metal. While 310 mm × 150 mm × 18 mm plates were placed face to face, FCAW (Flux-Cored Arc Welding) process was performed with a route interval of 10 mm and a groove angle of 45, and the shielding gas of 98%Ar-2%O_2 was used. The detailed welding conditions are shown in Table 2. Figure 2 shows the images of macrostructure for the test specimens after welding.

2.3. Observation of microstructure

To observe the microstructure through optical microscope, macro scope, and scanning electron microscope (SEM), we cut the specimens by the dimension of L 30 mm x W 20 mm × H 10 mm and performed etching with HCl 10 ml + $HNO_3$10 ml + Alcohol 10 ml + Glycerol solution after grinding and polishing. In addition, to do phase analysis through EBSD, we performed the test after polishing more than 1 h in 1um, 0.04 um colloidal silica.

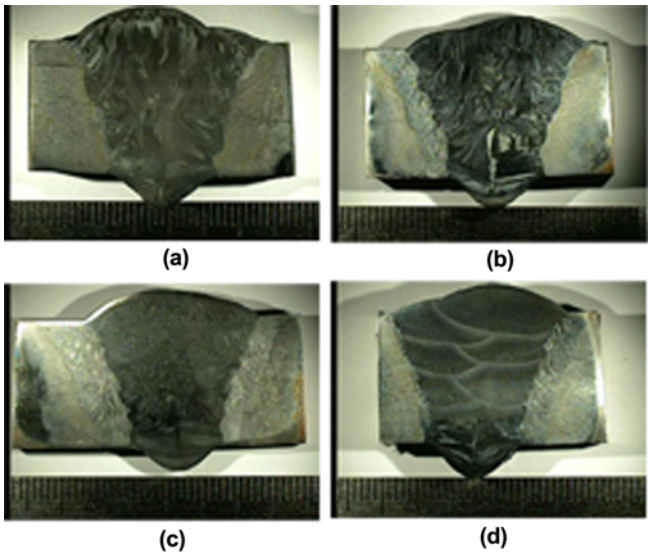

Fig. 2. Macrostructure of specimen. (a) No.1, (b) No.2, (c) No.3, and (d) No.4.

2.4. Corrosion test

To evaluate pitting resistance, we performed the potentiodynamic polarization test in 0.5M NaCl solution which was exhausted after injecting nitrogen more than 30 min, and to evaluate the degree of sensitization, we performed the DL-EPR (Double Loop Electrochemical Potentiokinetic Reactivation) test in 0.5 M H_2SO_4 + 0.01 M KSCN solution which had been proposed by Cihal and improved by Novak [14]. From the polarization curve obtained through each test, we calculated the pitting potential, E_{pit}. and used these as the index of pitting resistance and then evaluated the intergranular corrosion resistance by measuring the degree of sensitization (DOS) which is defined as the ratio (I_r/I_a) of maximum

Table 3. Results of polarization curves in 0.2 M H_2SO_4 solution

No.	E_{corr}	I_{crit}
1	-0.49 V	0.55×10^{-2}A/cm^2
2	-0.49 V	0.43×10^{-2}A/cm^2
3	-0.52 V	0.34×10^{-2}A/cm^2
4	-0.52 V	0.21×10^{-2}A/cm^2

Table 2. Welding parameters

Current (A)	Voltage (v)	Welding speed (CPM)	Heat input (KJ/mm)	Interlayer Temperature (°C)	Pass
200	26	8-16	2-4	120-140	8

anodic current density (I_a) when the potential rises in DL-EPR test to maximum anodic current density (I_r) when the potential falls. In the corrosion test, the working electrode was each specimen and the counter electrode was a platinum foil and the reference electrode was an Ag.AgCl/KCl-sat'd electrode.

3. RESULTS AND DISCUSSION

3.1. Pitting resistance

The materials, which form the passive film such as in stainless steel containing chrome and in nickel alloy, are sensitive especially to the pitting by local film destruction [17]. To evaluate the pitting resistance of the stainless steel weld metal which is sensitive to this pitting, we performed the polarization test in 0.5 M NaCl solution and the result is shown in Fig. 3. Polarization curve was illustrated in the pitting test, and the pitting potential and the corrosion potential measured through polarization curve were described in Table 4 in detail. For the passive area of each specimen, the pitting occurred after being measured to -0.13 V in No.1, -0.11 V in No.2, 0.19V in No.3, and 0.26V in No.4. As a result of analysis for measured polarization curve and pitting potential, between No.1 to which Ti and Nb were not added and No.2 to which only Ti was added, the pitting potential difference was 0.23V, and the pitting potential difference between No.2 and No.3 to which Ti and Nb were added was 0.30V. When the pitting potential difference of No.1 and No.2 was

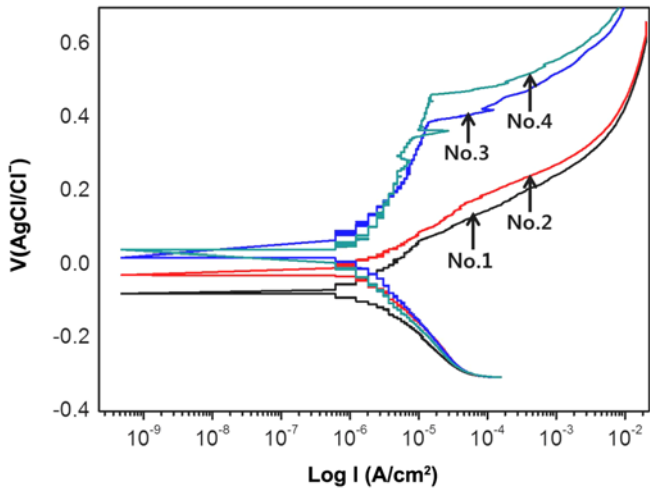

Fig. 3. Polarization curves in 0.5 M NaCl solution.

Table 4. Results of polarization curves in 0.5 M NaCl solution

No.	E_{corr}	E_{pit}
1	-0.26 V	-0.13 V
2	-0.20 V	-0.11 V
3	-0.17 V	0.19 V
4	-0.15 V	0.26 V

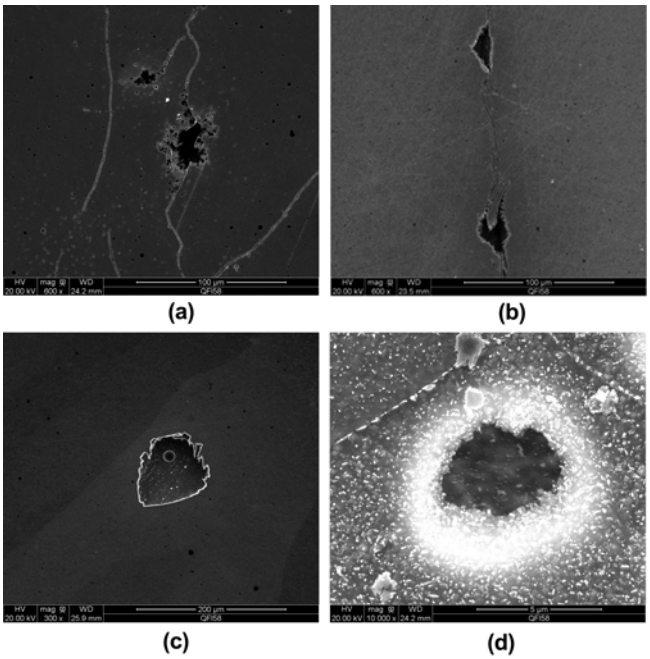

Fig. 4. SEM images of specimens after pitting corrosion test: (a) No.1, (b) No.2, (c) No.3, and, and (d) No.4.

compared with that of No.2 and No.3, the difference was found to be very big. No.4 with additional 0.5% Nb content showed 0.74V higher pitting potential than No.3. As a result, it is found that the pitting resistance increased more considerably when Ti and Nb were added together than when only Ti was added. Also, when the content of Nb was increased more, the pitting resistance increased. In general, it is known that the alloy elements, Cr, Mo, N, W, Si, V, Ni, can increase the pitting resistance of the stainless steel weld metal, but through this test result, it was identified that Ti and Nb also increased the pitting resistance effectively [10]. Figure 4 is SEM image observed from the time when the pitting occurred during the polarization test after the test was stopped. As a result of the observation on SEM image, for No.1 and No.2, the pitting occurred in the grain boundary and for No.3 and No.4, it was observed in the intercrystalline. As a result of the pitting test, it is found that the more the added contents of Ti and Nb increased, the higher the pitting corrosion was. And also it is found that the position which the pitting occurred was different with respect to the added contents of Ti and Nb.

3.2. Intergranular corrosion resistance

Figure 5 shows the result of DL-EPR test that was performed in 0.5 M H_2SO_4+KSCN 0.01 M to evaluate the intergranular corrosion resistance. All graphs show that big loops were observed as the potential rose, and when the potential fell again, small loops were observed only for No.1 and No.2. We measured the critical current density (I_a) which appears when the potential rises and the critical current density (I_r)

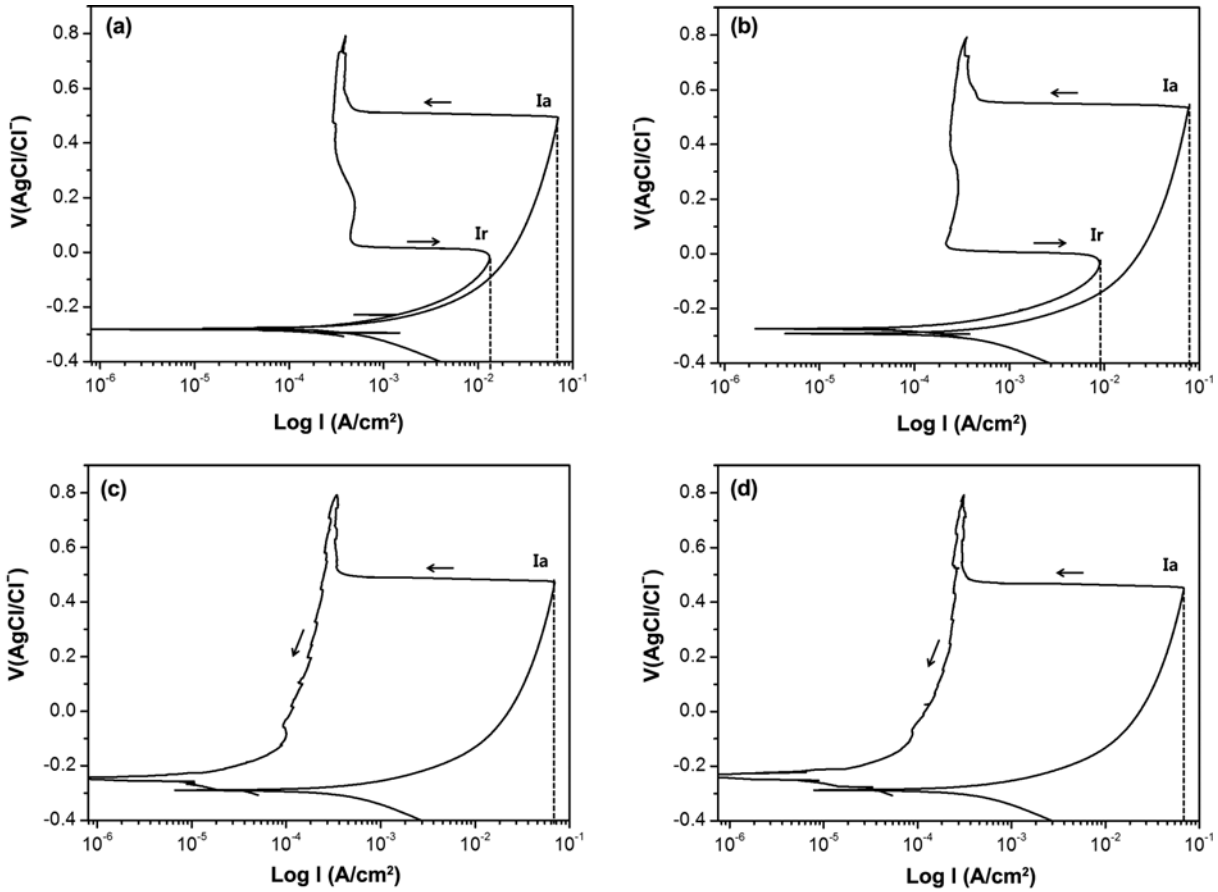

Fig. 5. DL-EPR curves in 0.5M H_2SO_4 + 0.01M KSCN: (a) No.1, (b) No.2, (c) No.3, and (d) No.4.

Table 5. Degree of sensitization

No.	I_a	I_r	DOS
1	0.69×10^{-1}A/cm^2	0.13×10^{-1}A/cm^2	18%
2	0.76×10^{-1}A/cm^2	0.09×10^{-1}A/cm^2	11%
3	0.69×10^{-1}A/cm^2	-	-
4	0.68×10^{-1}A/cm^2	-	-

when the potential falls. And we calculated the degree of sensitization (I_r/I_a), and the result was described in Table 5. I_a of each specimen generally showed the similar value, but I_r showed a big difference. No.1 was measured as 0.13×10^{-1}A/cm^2, and No.2 as 0.09×10^{-1}A/cm^2, but for No.3 and No.4, the critical current density was not measured as the loop was not observed when the potential fell. As a result of this, it is found that as the contents of Ti and Nb increased, I_r decreased and the degree of sensitization also decreased. Figure 6 shows microstructure and SEM taken after performing DL-EPR test. The image (a) is the Microstructure of a specimen without adding any stabilizing element such as Ti and Nb. And it shows that there was a considerable progress of the intergranular corrosion. On the other hand, the image of the Microstructure of a specimen in (b) where only Ti was added shows that less progression of the intergranular corrosion was observed than (a). In (c) and (d) where Ti and Nb were added together, the degree of the intergranular corrosion was much lower than both (a) and (b) because Ti, Nb, Zr and V are strong carbide-forming elements. When both Ti and Nb added, the stainless steel has been dual stabilized [13]. In addition, the addition of Nb above a 0.5 wt% did not greatly affect the intergranular corrosion.

3.3. Electron back scatter diffraction (EBSD) analysis

To identify the relation between the addition of Ti, Nb and the corrosion resistance, we observed the microstructure through EBSD. EBSD was used for this thesis as it is able to analyze the relatively wide range of the collective structure compared to Transmission Electron Microscope (TEM) and able to indicate as orientation, phase, and grain map etc. [18-19]. Figure 7 is the grain map for each specimen observed through EBSD. Each grain is indicated by each different color. The image (a) presents No.1 to which the stabilization elements Ti and Nb were not added, and the precipitation marked as white was formed in the grain boundary. As a result of the observation by Phase map, this precipitation was identified as Cr carbide. The image (b) presents No.2 to which only Ti

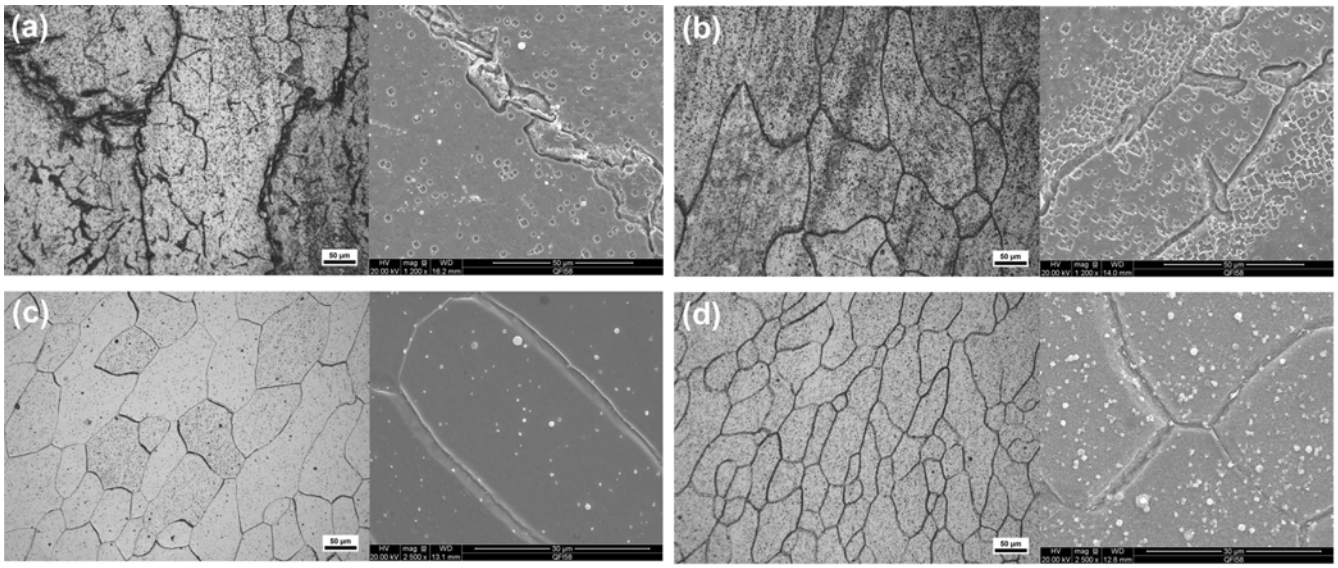

Fig. 6. Microstructure and SEM image of specimens after DL-EPR test: (a) No.1, (b) No.2, (c) No.3, and (d) No.4.

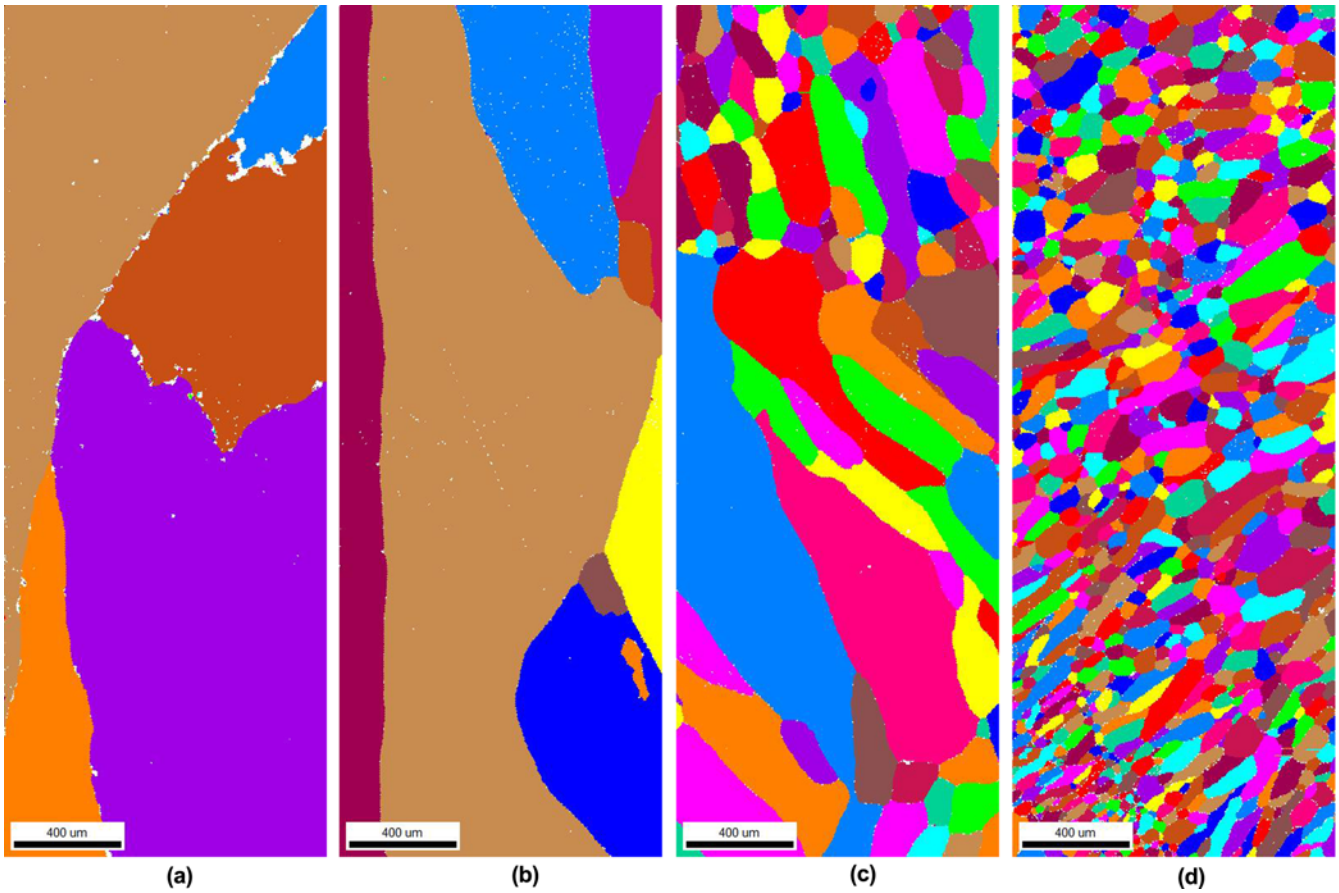

Fig. 7. Grain map of specimens by EBSD: (a) No.1, (b) No.2, (c) No.3, and (d) No.4.

was added. The amount of precipitation formed in the grain boundary is less than that of (a), but fine Cr carbide can be observed in intercrystalline and grain boundary. In the images of (c) and (d), as in (b), Cr carbide was observed in intercrystalline and grain boundary. Figure 8 is the result of the analysis through SEM/EDS. In the images of (a) and (b), as in

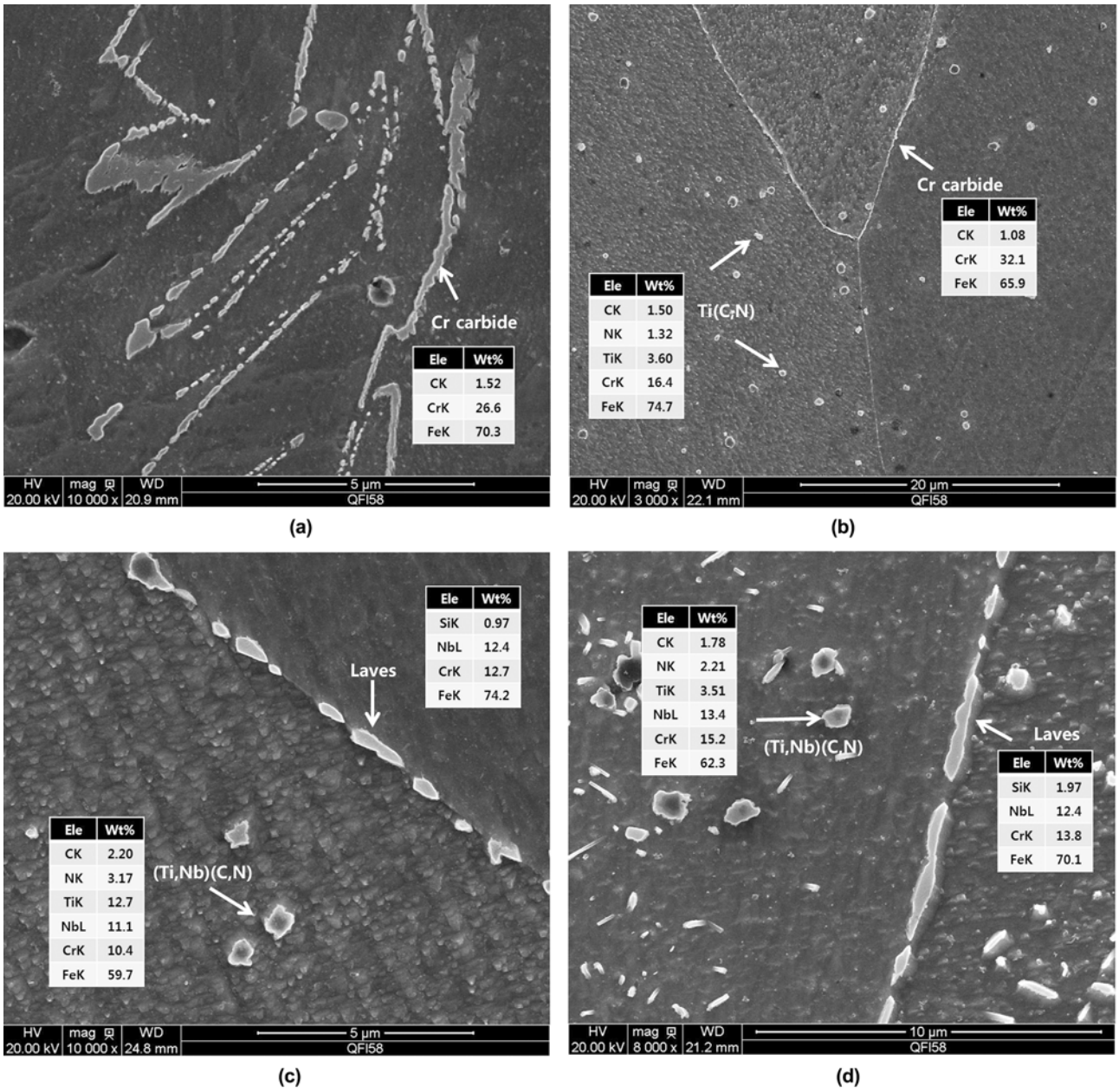

Fig. 8. SEM/EDS analysis of specimens: (a) No.1, (b) No.2, (c) No.3, and (d) No.4.

EBSD analysis, Cr carbide was observed, and in (b) where Ti was added, Ti carbide and nitride was observed. In (c) and (d) where Ti and Nb were added together, Ti and Nb carbide and nitride was observed. Laves phase was also observed at the grain boundary. As a result, As the contents of Ti and Nb increased, pitting and intergranular corrosion resistance increased, which result is related to the precipitation of Cr carbide. When chrome carbide is precipitated in the grain boundary of stainless steel, the area of Cr exhaustion is formed around the grain boundary, which is called sensitization. It has been reported that when stainless steel is sensitized like this, the intergranular corrosion occurs easily [12]. When Ti, Nb were not added, Cr carbide was precipitated around the grain boundary, and thus corrosion and pitting occurred first in the grain boundary which is relatively weak in the corrosion resistance. On the contrary, when the contents of Ti and Nb were increased, the precipitation of Cr carbide was prevented and the corrosion resistance was improved.

4. CONCLUSIONS

We prepared 4 specimens of the weld metal by adjusting the contents of Ti and Nb in the existing flux cored wire components for ferritic stainless steel of the automobile muf-

fler and evaluated pitting corrosion and intergranular corrosion resistance. The conclusion is as follows.

As a result of the pitting corrosion test in 0.5 M NaCl, it is found that the higher the contents of Ti and Nb increased, the more excellent the pitting resistance was. In addition, for the specimen to which Ti and Nb were not added, the pitting occurred in the grain boundary and when Ti and Nb were added, it occurred in the intercrystalline. In the DL-EPR test performed in 0.5M H_2SO_4 + 0.01M KSCN, the higher the contents of Ti and Nb increased, the lower I_r value decreased and thus the degree of sensitization decreased. Therefore, the cause of the increase of pitting and intergranular corrosion resistance was Cr carbide formed in the crystal grain boundary. And we have proved through EBSD that when Ti and Nb were added more, Cr carbide was formed less.

ACKNOWLEDGMENTS

This investigation was supported by the Dong-A University Research Fund.

REFERENCES

1. J. Jang and C. J. Park, *J. of Advanced Engineering and Technology* **3**, 333 (2010).
2. S. H. Lee, Y. T. Shin, and H. W. Lee, *Korean J. Met. Mater.* **50**, 280 (2012).
3. M. Sim and K. S. Lee, *Mater. Sci. Eng. A* **396**, 159 (2005).
4. Y. Song and Y. S. Ahn, *J. of KSPSE* **14**, 59 (2010).
5. G. Hong and K. B. Kang, *J. of KWJS* **27**, 79 (2009).
6. C. Lee and B. Y. Lee, *J. of KWJS* **27**, 27 (2009).
7. T. J. Park, J. P. Kong, H. S. Na, C. Y. Kang, S. H. Uhm, J. K. Kim, I. S. Woo and J. S. Lee, *J. of KWJS* **28**, 92 (2010).
8. K. H. Kim, K. H. Do, W. J. Choi, S. B. Lee, D. S. Kim, and J. J. Pak, *Korean J. Met. Mater.* **51**, 113 (2013).
9. D. Y. Ryoo, S. H. Park, and M. N. Park, *J. of KIMM* **34**, 207 (1996).
10. A. J. Sedriks, *Corrosion of Stainless Steels, 2nd ed*., pp. 45-46, pp.121-122, John Wiley & Sons, New York (1996).
11. S. Kou, *Welding Metallurgy, 2nd ed*., pp.447-448, John Wiley & Sons, New York (2003).
12. J. C. Lippold and D. J. Kotecki, *Welding Metallurgy and Weldability of Stainless Steels*, pp.126-130, John Wiley & Sons, New York (2005).
13. H. Yan, H. Bi, X. Li, and Z. Xu, *Mater. Charact*. **59**, 1741 (2008).
14. U. S. Hwang and Y. D. Lee, *J. of KWJS* **2**, 189 (2000).
15. L. X. Wang and Q. J. Zhai, *Mater. Design* **30**, 49 (2009).
16. J. Sedriks, *Corrosion of Stainless Steels, 2nd ed*., pp.45-46, pp.239-242, John Wiley & Sons, New York (1996).
17. D. A. Jones, *Principles and Prevention of Corrosion, 2nd ed.*, pp.32-34, Prentice Hall, United States (1995).
18. V. Randle and O. Engler, *Introduction to Texture Analysis: Macrotexture, Microtexture and Orientation Mapping*, pp. 125-203. CRC Press, New York (2000).
19. R. A. Schwarzer, D. P. Field, B. L. Adams, M. Kumar, and A. J. Schwartz, *Electron Backscatter Diffraction in Materials Science*, 2nd ed., (eds. A. J. Schwartz, M. Kumar, B. L. Adams, D. P. Field), pp.1-20, Springer, New York (2009).